JOURNAL OF SOFT COMPUTING AND DATA MINING
e-ISSN: 2716-621X

JSCDM

Vol. 6 No. 3 (2025) 219-242
https://publisher.uthm.edu.my/ojs/index.php/jscdm

A Comparative Study of Filter-Based Feature Selection in High-Dimensional Medical Datasets Using Whale Optimization Variants

Li Yu Yab[1], Noorhaniza Wahid[1]*, Rahayu A Hamid[1], José Machado[2]

[1] *Faculty of Computer Science and Information Technology, Universiti Tun Hussein Onn Malaysia, Parit Raja 86400, Johor, MALAYSIA*

[2] *ALGORITMI Center, Departamento de Informática, Universidade do Minho, Campus of Gualtar, Braga 4710-057, PORTUGAL*

*Corresponding Author: nhaniza@uthm.edu.my
DOI: https://doi.org/10.30880/jscdm.2025.06.03.015

Article Info

Received: 16 August 2025
Accepted: 7 November 2025
Available online: 30 December 2025

Keywords

Filter-based feature selection, hierarchical whale optimization algorithm, metaheuristic optimization, high-dimensional data, microarray gene expression

Abstract

High-dimensional medical datasets, such as microarray gene expression profiles, pose significant challenges for feature selection (FS) due to their large feature space and limited sample size, often resulting in unstable and inconsistent outcomes. Metaheuristic algorithms like the Whale Optimization Algorithm (WOA) have shown promise in FS; however, their reliance on a single leader and linear control parameter typically leads to poor exploration-exploitation balance and reduced stability. This study proposes a Hierarchical Whale Optimization Algorithm (HiWOA) for filter-based FS, incorporating two key enhancements: a hierarchical leadership strategy, where three leaders guide the search, and an arcsine-based control parameter that enables a smoother transition between exploration and exploitation. Unlike earlier HiWOA applications in optimization or wrapper-based selection, this is the first to adapt HiWOA to filter-based FS. Experiments were conducted on five benchmark medical datasets using four filter methods (ANOVA, Chi-square, Mutual Information, and Pearson Correlation), with performance evaluated in terms of algorithmic stability, FS stability, and classification accuracy using kNN. Results demonstrate that HiWOA consistently achieves well-balanced exploration-exploitation ratio with higher exploration rates (+25.66%), improved FS stability (+0.00261 in MKCI), and superior classification accuracy (+11.28%) compared to WOA and its variants. Among the filter methods, ANOVA combined with HiWOA delivered the most discriminative feature subsets, establishing a robust framework for high-dimensional medical data analysis.

1. Introduction

High-dimensional datasets, particularly microarray gene expression data, pose significant challenges in medical data analysis [1]. These datasets often contain thousands of attributes but only a limited number of samples, making classification unstable and prone to overfitting [2]. Such complexity requires dimensionality reduction techniques to improve computational efficiency and ensure reliable diagnostic outcomes [3].

Feature Selection (FS) has been widely adopted to address these challenges by identifying the most relevant attributes while discarding less informative ones [3]. FS not only reduces dimensionality but also enhances

interpretability and classification accuracy across diverse domains, ranging from cancer diagnosis [4] to phishing detection [5]. Broadly, FS methods are categorized into filter, wrapper, and embedded approaches, each with distinct strengths: Filter methods are computationally efficient, wrapper methods provide strong predictive power but are resource-intensive, and embedded methods integrate FS within the learning process [6]. In medical datasets, filter-based methods are often preferred over wrapper or embedded methods not only for their computational efficiency but also because they are independent of classifier bias and more suitable for small-sample, high-feature scenarios that commonly occur in biomedical studies [7].

In recent years, metaheuristic optimization algorithms have been increasingly applied to FS due to their flexibility in exploring large search spaces [8]. Genetic Algorithms, Particle Swarm Optimization, Grey Wolf Optimizer (GWO), and other swarm intelligence techniques have been successfully applied in domains such as text mining, biomedical classification, and multi-label learning [9–11]. The Whale Optimization Algorithm (WOA), inspired by humpback whale foraging behavior, has also gained attention for FS tasks [12–14]. However, standard WOA suffers from two limitations: its reliance on a single leader and its linear control parameter, which leads to instability in both algorithmic balance and FS outcomes [15]. Stability is particularly important in high-dimensional medical datasets, where inconsistent algorithmic behavior or unstable feature subsets may result in unreliable classifications and reduced reproducibility of findings.

To overcome these issues, this paper proposes a Hierarchical Whale Optimization Algorithm (HiWOA) for filter-based FS. HiWOA introduces a hierarchical leadership structure with three guiding agents that is inspired from GWO and replaces the linear control parameter with an arcsine-based decreasing function to achieve a smoother balance between exploration and exploitation. While it has previously been explored in optimization and wrapper-based contexts, this is the first study to extend it to filter-based FS in high-dimensional medical datasets.

The contributions of this study are summarized as follows:

- A comparative evaluation of five WOA variants, namely standard WOA, Enhanced WOA (EWOA), Opposition-Based Whale Optimization Algorithm (OWOA), mWOA, and the proposed HiWOA, applied to solve stability problems of high-dimensional FS.
- Extensive experiments on five benchmark medical datasets (RNA-Seq, Lung, Lymphoma, SRBCT, and Colon) using four filter-based FS methods (ANOVA, Chi-square, Mutual Information, and Pearson Correlation Coefficient).
- A multi-criteria performance assessment covering (a) algorithmic stability in terms of exploration-exploitation balance, (b) FS stability measured with the Modified Kuncheva Consistency Index, and (c) classification accuracy obtained with kNN.
- An important finding that the combination of HiWOA with ANOVA is the most promising choice, as it consistently produced discriminative features with high classification accuracy, while also maintaining acceptable levels of algorithmic balance and FS stability.

The remainder of this paper is organized as follows. Section 2 reviews related works on FS and metaheuristic algorithms, with particular focus on WOA and its variants. Section 3 describes the materials and methods, including datasets, filter-based criteria, WOA variants, and evaluation metrics. Section 4 reports and discusses the experimental results in terms of algorithmic stability, FS stability, and classification accuracy. Finally, Section 5 concludes the paper with a summary of findings and directions for future work.

2. Related Work

This section reviews existing WOA variants that are most relevant to this study. Sections 2.1 to 2.3 describe EWOA, mWOA, and OWOA, respectively. Lastly, a comparative summary of these algorithms is provided in Section 2.4.

2.1 Enhanced WOA (EWOA)

The EWOA proposed by Reddy and Saha modified several position update equations and introduced changes to the algorithmic structure [16]. By integrating additional stochastic terms, adaptive coefficients, and fragments from the Artificial Bee Colony algorithm, EWOA improved both convergence rate and exploitation ability. It consistently achieved superior results on the CEC2019 benchmark functions and engineering design problems. Despite demonstrating faster convergence and better accuracy, the analysis of stability was restricted to convergence trends, without systematic evaluation of exploration-exploitation balance. Its improvements have yet to be validated in solving FS problems.

2.2 Modified WOA (mWOA)

The mWOA was developed specifically for filter-based FS on high-dimensional datasets [17]. The modification centered on the control parameter, a, which was changed from a linearly decreasing to a linearly increasing

function. This straightforward adjustment allowed the algorithm to switch positions more rapidly in early iterations, improving exploration and convergence speed. It was implemented as a filter-based FS method, using a Euclidean distance-based fitness function to evaluate the distance of feature mean values across binary classes, thereby determining each feature's discriminative power. The mWOA was tested on four benchmark medical datasets and demonstrated competitive classification accuracy. While it improved convergence speed and accuracy, the study only evaluated the proposed method against the standard WOA and a no-feature-selection setting, which provides limited comparative insight.

2.3 Opposition-Based Whale Optimization Algorithm (OWOA)

OWOA augments the standard WOA with opposition-based learning during initialization and position updates throughout iterations, where each candidate is evaluated alongside its opposite [18]. This enlarges search coverage, accelerates early exploration, and helps escape local optima. Reported benefits focus on faster convergence and improved solution quality across benchmarks, including applications such as the optimal power flow problem. However, prior work typically does not provide a systematic analysis of stability. The enhancements introduced have primarily been evaluated on optimization tasks, yet the applicability to FS tasks is still to be confirmed.

2.4 Comparison of WOA variants

Table 1 summarizes the reviewed WOA variants in terms of their modifications and contributions.

Table 1 *Summary of WOA variants*

Algorithm	Modification	FS	Main Objective	Reported Strengths	Limitation
EWOA [16]	Modified update equations, adaptive coefficients, ABC component	None	Improve convergence rate and exploitation	Faster convergence, superior accuracy on benchmarks	Focus on accuracy, stability not systematically evaluated
mWOA [17]	Control parameter, a, changed to linearly increasing	Filter-based	Improve exploration and convergence speed	Better FS accuracy on high-dimensional data	Did not analyze exploration, exploitation or FS subset stability
OWOA [18]	Opposition-based learning in initialization and position update	None	Improve exploration and convergence	Better coverage, quicker escape from local optima	Stability across runs and FS consistency rarely evaluated

From these studies, it is clear that prior WOA modifications mainly emphasize convergence speed and classification accuracy. However, both algorithmic stability (exploration-exploitation balance) and FS stability (consistency of selected subsets) remain underexplored. To bridge this gap, the present work proposes HiWOA for filter-based FS and conducts a comprehensive comparative study of stability and classification performance on multiple medical datasets.

3. Materials and Methods

This section presents the materials and methods used in this study. It begins with a description of five high-dimensional medical datasets, followed by an overview of the four filter-based FS methods that serve as fitness functions. The five search algorithms, consisting of the standard WOA, three of its variants, and the proposed HiWOA, are then outlined. Finally, the section explains the evaluation metrics used to assess algorithmic stability, FS stability, and classification performance, as well as the experimental settings applied.

3.1 Datasets

Table 2 presents the high-dimensional datasets used in this study, arranged in descending order of feature size. The column 'Dataset' lists the dataset name, while '#Instances' denotes the number of samples (observations) and '#Features' indicates the number of attributes (genes). The column 'Classes' specifies the number of target categories, whereas 'Type' refers to the data format, and lastly, 'Source' identifies where the dataset was obtained.

Table 2 *Characteristics of benchmark medical datasets*

Datasets	#Instances	#Features	Classes	Type	Source
RNA-Seq	801	20531	5	Numerical	[19]
Lung	203	12600	5	Numerical	[20]
Lymphoma	47	4026	2	Numerical	[21]
SRBCT	83	2308	4	Numerical	[22]
Colon	62	2000	2	Numerical	[23]

The RNA-Seq dataset contains gene expression profiles of 801 cancer patients across 20,531 genes, spanning five tumor classes (BRCA, COAD, KIRC, LUAD, and PRAD). The Lung dataset includes 203 samples with 12,600 genes and five classes (adenocarcinoma, normal lung tissue, small-cell carcinoma, squamous carcinoma, and carcinoid). The Lymphoma dataset comprises 47 samples and 4,026 genes across binary classes (24 Germinal Centre B-like samples and 23 Activated B-like samples). The SRBCT dataset has 83 samples with 2,308 genes divided into four classes (Ewing's sarcoma, Burkitt's lymphoma, neuroblastoma, rhabdomyosarcoma). Finally, the Colon dataset includes 62 samples with 2,000 genes across tumor and normal classes. These datasets differ in size, class distribution, and complexity, providing diverse benchmarks for evaluating filter-based FS methods.

3.2 Filter-based FS Methods

In this study, four widely used filter-based FS methods were adopted as fitness functions to evaluate the relevance of features with respect to the class labels. These methods were chosen because they are computationally efficient, independent of classification models, thus suitable for high-dimensional medical datasets [24].

Let the dataset have d features and class labels Y. For a candidate subset, $S \subseteq \{1, \dots, d\}$, define a per-feature relevance score, $S_j \in [0,1]$ from one of the filters below. The aggregate subset quality is the mean score of per-feature relevance score in that subset, as shown in Eq. (1). Next, a minimize cost function is used as shown in Eq. (2) where the first weight, α, emphasizes feature relevance, and the second weight, β, penalizes subset size. Hence, the smaller the fitness value, $\bar{s}(S)$, the better the solution is.

$$\bar{s}(S) = \frac{1}{|S|}\sum_{j\in S} S_j \tag{1}$$

$$J(S) = \alpha\big(1 - \bar{s}(S)\big) + \beta\frac{|S|}{d}, \qquad \alpha, \beta \geq 0, \alpha + \beta = 1 \tag{2}$$

Since this study compares 4 different filter-based FS methods, each method was implemented as a separate fitness function. Let j denote different filter-based methods, then, for a selected subset of features, the feature relevance score, S_j, is computed using one of the following measures.

3.2.1 Analysis of Variance (ANOVA)

ANOVA is a statistical test that measures whether the mean values of a feature differ significantly across multiple classes [24]. Features with higher F-statistics, F_j, are considered more discriminative. Eq. (3) models the ANOVA F-statistics, where k indicates number of groups (i.e., number of classes in the dataset), c indicates the index for each group, n_c is the number of samples in c group, $\overline{x}_{jc}$ is the mean value of feature j in c group, $\overline{x}_j$ is the overall mean of feature j across all samples, i is the index of individual samples within a group, x_{ji} is the value of feature j for sample i, MSB (Mean Square Between) is the Sum of Squares Between groups over $k-1$, and MSW (Mean Square Within) is the Sum of Squares Within groups over $N-k$. Then, the S_j is computed as bounded in 0 to 1 as shown in Eq. (4).

$$F_j = \frac{MSB_j}{MSW_j} = \frac{\frac{1}{k-1}\sum_{c=1}^{k} n_c(\overline{x}_{jc} - \overline{x}_j)^2}{\frac{1}{N-k}\sum_{c=1}^{k}\sum_{i\in c}(x_{ji} - \overline{x}_{jc})^2} \tag{3}$$

$$S_j = \frac{F_j}{F_j + 1} \in [0,1] \tag{4}$$

3.2.2 Chi-square

Chi-square score, χ^2 , is a non-parametric test that evaluates the independence between categorical class labels and individual features [24]. A higher Chi-square score indicates stronger association between the feature and the

J. of Soft Computing and Data Mining Vol. 6 No. 3 (2025) p. 219-242

target class. Eq. (5) models the Chi-square statistic test to evaluate whether a feature X and the class label Y are independent., where i is the index for feature categories, c is the index for the class labels, O_{ic} (Observed frequency) is the actual number of samples where feature X takes category i and belongs to class c, and E_{ic} (Expected frequency) is the product of (row total for i) and (column total for c) divided by the total. Lastly, Eq. (6) normalizes the score to [0,1].

$$\chi_j^2 = \sum_i \sum_c \frac{(O_{ic} - E_{ic})^2}{E_{ic}} \tag{5}$$

$$S_j = \mathcal{N}(\chi_j^2) \in [0,1] \tag{6}$$

3.2.3 Mutual Information

Mutual Information is an information-theoretic measure that quantifies the amount of shared information between a feature and the class label [24]. Features with high scores are more informative in predicting the outcome. Eq. (7) models the Mutual Information, MI, where x is a possible value (discrete bin) of the feature X, y is a possible value (class label) of Y, $p(x,y)$ is the joint probability that feature X takes value x and the class label is y, $p(x)$ is the marginal probability that feature X takes value x regardless of class, and $p(y)$ is the marginal probability that class label Y is y regardless of feature. Then, Eq. (8) normalizes the score to [0,1].

$$MI(X_j;Y) = \sum_x \sum_y p(x,y) \log \frac{p(x,y)}{p(x)\,p(y)} \tag{7}$$

$$S_j = \mathcal{N}(MI(X_j;Y)) \in [0,1] \tag{8}$$

3.2.4 Pearson Correlation Coefficient

Pearson Correlation Coefficient, r, is a linear correlation measure that assesses the strength of association between a feature and the class label [24]. Features with higher absolute correlation values are prioritized. Eq. (9) models the Pearson Correlation Coefficient where $\text{cov}(X_j, Y)$ is the covariance between feature X and class label Y to assess how much they vary together, σ_{X_j} is the standard deviation of X, and σ_Y is the standard deviation of Y. Eq. (10) ensures the computed correlation values stay absolute within 0 to 1.

$$r_j = \frac{\text{cov}(X_j, Y)}{\sqrt{\sigma_{X_j}\sigma_Y}} \tag{9}$$

$$S_j = |r_j| \in [0,1] \tag{10}$$

In short, each of these filter-based FS method was used independently as a fitness function during the search process. By comparing across multiple methods, this study provides a more comprehensive evaluation of how different statistical measures of relevance affect FS stability and classification accuracy.

3.3 Search Algorithms

This section describes the search algorithms employed in this study, including the standard WOA, its variants, and the proposed HiWOA.

3.3.1 Whale Optimization Algorithm (WOA)

WOA is a swarm-based metaheuristic inspired by the bubble-net hunting strategy of humpback whales [25]. It has been widely applied to optimization and FS problems due to its simplicity and effectiveness. WOA has three behaviors: encircling mechanism, exploitation via Bubble-Net attacking, and exploration via searching for prey. Fig. 1 depicts the Bubble-Net attacking of WOA.

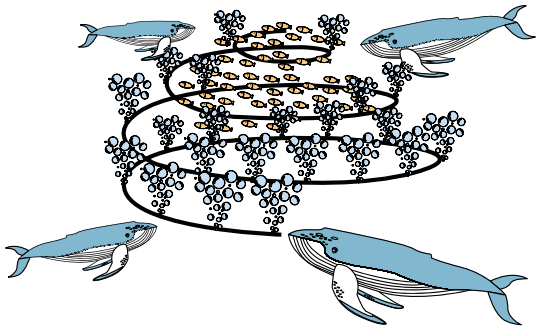

Fig. 1 *WOA's Bubble-Net attacking mechanism*

In its encircling mechanism, whales approach the prey by updating their positions relative to the best-known solution. The update rule is expressed in Eq. (11), where $\overrightarrow{X^*}$ represents the position of the current best solution, t indicates the iteration index, $\vec{A}$ is a coefficient vector defined in Eq. (12), and $\vec{D}$ indicates the distance between the whale and its prey calculated by Eq. (13). The control parameter a decreases linearly over iterations as shown in Eq. (14), while $\vec{C}$ in Eq. (15) depends on a random vector, $\vec{r}$.

$$\vec{X}(t+1) = \overrightarrow{X^*}(t) - \vec{A} \cdot \vec{D} \tag{11}$$

$$\vec{A} = 2\vec{a} \cdot \vec{r} - \vec{a} \tag{12}$$

$$\vec{D} = |\vec{C} \cdot \overrightarrow{X^*}(t) - \vec{X}(t)| \tag{13}$$

$$a = 2 - t(2/MaxIter) \tag{14}$$

$$\vec{C} = 2 \cdot \vec{r} \tag{15}$$

The exploitation capability of WOA is driven by a bubble-net feeding method, which combines both shrinking encirclement and spiral updating. The spiral mechanism models a whale's helical path around its prey, formulated in Eq. (16), where the distance $\vec{D}$ is defined in Eq. (17). The strategy applied depends on a probability factor p: when $p < 0.5$, the encircling Eq. (11) is used, otherwise the spiral update Eq. (16) is applied.

$$\vec{X}(t+1) = \vec{D} \cdot e^{bl} \cdot \cos(2\pi l) + \overrightarrow{X^*}(t) \tag{16}$$

$$\vec{D} = |\overrightarrow{X^*}(t) - \vec{X}(t)| \tag{17}$$

During exploration, whales diversify the search by moving relative to randomly selected individuals in the population. When $|\vec{A}| \geq 1$, the position is updated using Eq. (18), where $\overrightarrow{X_{rand}}$ represents the location of the randomly chosen whale and $\vec{D}$ is obtained from Eq. (19). For $|\vec{A}| < 1$, the algorithm transitions from exploration to exploitation.

$$\vec{X}(t+1) = \overrightarrow{X_{rand}} - \vec{A} \cdot \vec{D} \tag{18}$$

$$\vec{D} = |\vec{C} \cdot \overrightarrow{X_{rand}} - \vec{X}| \tag{19}$$

The overall procedure of the standard WOA is summarized in the pseudocode shown in Fig. 2.

```
Initialize the whale population X_i (i = 1, 2, ..., n)
Calculate the fitness of each search agent
Assign the best search agents as X*
While (t < maximum number of iterations)
    for each search agent
        Update a, A, C, l, and p with Eq. (14), Eq. (12), Eq. (15), [-1,1], [0,1] respectively
        if (p < 0.5)
            if (|A| < 1)
                Update the position of the current search agent by Eq. (11)
            else
                Select a random search agent as X_rand
                Update the position of the current search agent by Eq. (18)
            end if
        else
            Update the position of the current search by Eq. (16)
        end if
    end for
    Check if any search agent goes beyond the search space and amend it
    Calculate the fitness of each search agent
    Update the best search agents as X*
    t = t + 1
end while
return X*
```

Fig. 2 *Pseudocode of the standard WOA*

3.3.2 WOA Variants

Several variants of WOA have been introduced in the literature to enhance its performance in different optimization contexts. In this study, three representative variants are considered: the Enhanced WOA (EWOA), the Modified WOA (mWOA), and the Opposition-Based WOA (OWOA). Their main principles and contributions were discussed in Section 2 (Related Works). While these algorithms report improvements in convergence and solution quality, their stability in terms of exploration-exploitation balance and FS consistency has not been explicitly examined. Therefore, they are included here for comparative evaluation.

3.3.3 Proposed HiWOA

The proposed Hierarchical Whale Optimization Algorithm (HiWOA) extends the standard WOA by introducing two main modifications. First, instead of relying on a single leader, X^*, HiWOA employs a hierarchical leadership structure with three guiding agents: alpha X_α, beta X_β, and delta X_δ, as inspired by GWO [26]. Having multiple leaders allows search agents to update their positions relative to multiple leaders, improving diversity and reducing the risk of premature convergence [27]. To implement the hierarchical leadership structure, Eq. (20) is used to replace both the encircling Eq. (11) and the spiral update Eq. (16).

$$\vec{X}(t+1) = \frac{\left(\overrightarrow{X_1} + \overrightarrow{X_2} + \overrightarrow{X_3}\right)}{3} \tag{20}$$

When $p < 0.5$, the algorithm carries out encircling mechanism, hence, Eq. (21) to Eq. (23) are used to interpret the $\overrightarrow{X_1}$, $\overrightarrow{X_2}$, and $\overrightarrow{X_3}$ in Eq. (20).

$$\overrightarrow{X_1} = \overrightarrow{X_\alpha}(t) - \vec{A} \cdot \overrightarrow{D_\alpha} \text{ where } \overrightarrow{D_\alpha} = \left|\vec{C} \cdot \overrightarrow{X_\alpha} - \overrightarrow{X_t}\right| \tag{21}$$

$$\overrightarrow{X_2} = \overrightarrow{X_\beta}(t) - \vec{A} \cdot \overrightarrow{D_\beta} \text{ where } \overrightarrow{D_\beta} = \left|\vec{C} \cdot \overrightarrow{X_\beta} - \overrightarrow{X_t}\right| \tag{22}$$

$$\overrightarrow{X_3} = \overrightarrow{X_\delta}(t) - \vec{A} \cdot \overrightarrow{D_\delta} \text{ where } \overrightarrow{D_\delta} = |\vec{C} \cdot \overrightarrow{X_\delta} - \overrightarrow{X_t}| \tag{23}$$

On the contrary, when $p \geq 0.5$, the algorithm enters spiral update mechanism, Eq. (24) to Eq. (26) are used to interpret the $\overrightarrow{X_1}$, $\overrightarrow{X_2}$, and $\overrightarrow{X_3}$ in Eq. (20) instead.

$$\overrightarrow{X_1} = \overrightarrow{D_\alpha} \cdot e^{bl} \cdot \cos(2\pi l) + \overrightarrow{X_\alpha}(t) \text{ where } \overrightarrow{D_\alpha} = \left|\overrightarrow{X_\alpha} - \overrightarrow{X_t}\right| \tag{24}$$

$$\overrightarrow{X_2} = \overrightarrow{D_\beta} \cdot e^{bl} \cdot \cos(2\pi l) + \overrightarrow{X_\beta}(t) \text{ where } \overrightarrow{D_\beta} = \left|\overrightarrow{X_\beta} - \overrightarrow{X_t}\right| \tag{25}$$

$$\overrightarrow{X_3} = \overrightarrow{D_\delta} \cdot e^{bl} \cdot \cos(2\pi l) + \overrightarrow{X_\delta}(t) \text{ where } \overrightarrow{D_\delta} = \left|\overrightarrow{X_\delta} - \overrightarrow{X_t}\right| \tag{26}$$

Second, the control parameter, a, is adapted using an arcsine-based decreasing function, replacing the linear strategy from the standard WOA. The choice of arcsine was motivated by findings in a recent study on the exploration-exploitation trade-off in WOA, where several strategies such as cosine, sine, exponential, logarithmic, and arcsine were compared, and arcsine was reported to yield the most effective balance [28]. Also, nonlinear control strategy enables a smoother and more flexible transition between exploration and exploitation [15]. Hence, o model the changes, Eq. (14) is replaced by Eq. (27).

$$a = 2 - \left[2 \arcsin\left(\frac{t}{maxiter}\right) / \arcsin(1)\right] \tag{27}$$

In terms of computational complexity, the proposed HiWOA maintains the same asymptotic order as the standard WOA, i.e., $O(N \times D \times T)$, where N denotes the population size, D the number of features, and T the number of iterations. The introduction of three leaders and the arcsine-based control parameter adds only a constant computational overhead, which does not significantly affect runtime performance, because:

- 3 leaders instead of 1, only adds constant factor, i.e., × 3.
- arcsine-based control parameter replaces a linear update, still computed in constant time per iteration.
- no additional nested loops.

The idea of modifying the control parameter is not unique to this study. For instance, one of the WOA variants, mWOA, also introduces a modification to its control parameter. Fig. 3 illustrates a comparison of the control parameter in standard WOA, mWOA, and the proposed HiWOA.

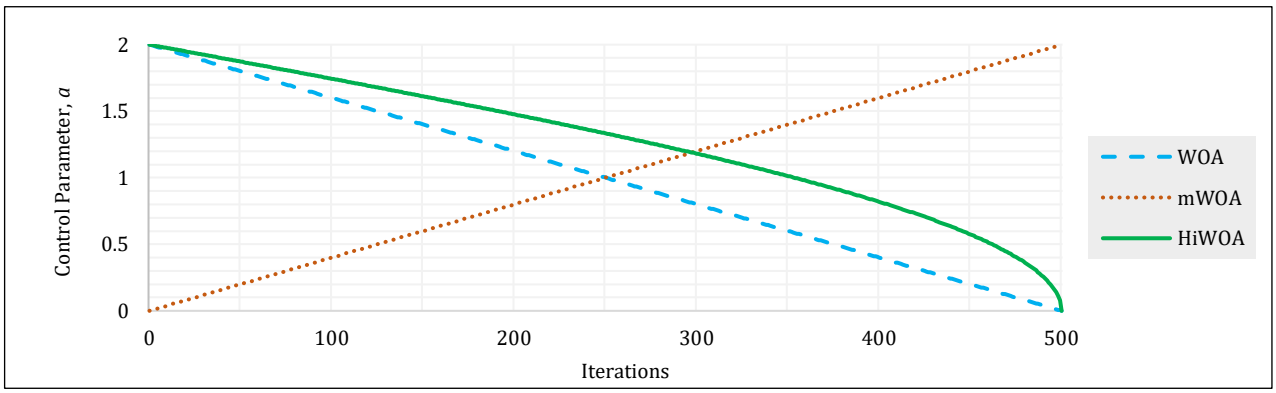

Fig. 3 *Comparison of the control parameter strategy in standard WOA, mWOA, and the proposed HiWOA*

In conclusion, by adopting multi-leader hierarchy structure, HiWOA promotes diversity, thus, resulting in higher exploration and possibility in finding better solution, while the arcsine-based control parameter ensures a smoother transition between exploration and exploitation for better algorithmic stability. As a result, HiWOA is expected to select more reliable feature subsets compared to the other WOA variants. The overall procedure of the proposed HiWOA is summarized in the pseudocode shown in Fig. 4.

```
Initialize the whale population X_i (i = 1, 2, ..., n)
Calculate the fitness of each search agent
Assign the top three search agents as X_∝, X_β , and X_δ
While (t < maximum number of iterations)
    for each search agent
        Update a, A, C, l, and p with Eq. (27), Eq. (12), Eq. (15), [-1,1], [0,1] respectively
        if (p < 0.5)
            if (|A| < 1)
                Update the position of the current search agent by Eq. (20) using Eq. (21) to Eq. (23)
            else
                Select a random search agent as X_rand
                Update the position of the current search agent by Eq. (18)
            end if
        else
            Update the position of the current search by Eq. (20) using Eq. (24) to Eq. (26)
        end if
    end for
    Check if any search agent goes beyond the search space and amend it
    Calculate the fitness of each search agent
    Update the top three search agents as X_∝, X_β , and X_δ
    t = t + 1
end while
return X_∝
```

Fig. 4 *Pseudocode of the proposed HiWOA*

3.4 Evaluation Metrics

To provide a comprehensive assessment of the search algorithms, three evaluation metrics were employed: algorithmic stability, FS stability, and classification accuracy. These metrics capture different aspects of performance, ranging from the internal search behavior of the algorithms to the quality and reliability of the selected feature subsets.

3.4.1 Algorithmic Stability

Algorithmic stability reflects the balance between exploration and exploitation throughout the optimization process [15]. A well-balanced search is important to avoid excessive exploitation or exploration. The stability of each algorithm was assessed by measuring the relative proportion of exploration and exploitation during the optimization process and then averaging these values over multiple runs. Eq. (28) computes the diversity in all dimensions, let dimension equal to number of features in the dataset, median(x^j) equals to the median of dimension j, and x_i^j indicates the dimension j of individual i in n population. Then, the diversity across dimensions is calculated in Eq. (29). Subsequently, the exploration and exploitation percentages are computed using Eq. (30) and Eq. (31), respectively.

$$Div_j = \frac{1}{n}\sum_{i=1}^{n} \text{median}(x^j) - x_i^j \tag{28}$$

$$Div = \frac{1}{D}\sum_{j=1}^{D} Div_j \tag{29}$$

$$Exploration\% = \frac{Div}{Div_{max}} \times 100\% \tag{30}$$

$$Exploitation\% = \frac{|Div - Div_{max}|}{Div_{max}} \times 100\% \tag{31}$$

3.4.2 Feature Selection Stability

FS stability evaluates the consistency of the selected subsets across multiple independent runs of the same algorithm. Inconsistent selection can reduce confidence in the chosen features, especially in high-dimensional

medical datasets. To quantify this, the modified Kuncheva's Consistency Index (MKCI) [29] was used. This index measures the degree of overlap between pairs of feature subsets, averaged across all runs, with higher values indicating more stable FS behavior. Eq. (32) calculates the pairwise MKCI between experiments E_1 and E_2, where r denotes the amount of overlap features selected from experiments E_1 and E_2, n indicates the total features in dataset, k_1 is the number of features selected from E_1, and k_2 is the number of features selected from E_2. Next, Eq. (33) computes the average MKCI values obtained from all the possible pairwise combinations in 30 experiments, thus, a total of $C(30,2) = 435$ pairs of feature subsets to compute.

$$MKCI(E_1, E_2) = \frac{rn - k_1 k_2}{k_2(n - k_1)}, \qquad k_2 < k_1 \tag{32}$$

$$Average\ MKCI = \frac{1}{C(30,2)} \sum_{i=1}^{C(30,2)} MKCI_i \tag{33}$$

3.4.3 Classification Accuracy

Ultimately, the quality of the selected features must be validated in terms of their predictive power. The classification accuracy of the reduced feature sets was measured using the k-Nearest Neighbors (kNN) classifier. Accuracy was computed as the percentage of correctly classified samples over all test cases using Eq. (34) [30], where TP and TN indicate the correctly classified positive and negative samples, while FP and FN denote the wrongly classified positive and negative samples. Since accuracy directly reflects the discriminative strength of the selected features, it serves as a practical indicator of the effectiveness of each method.

$$Accuracy = \frac{TP + TN}{TP + TN + FP + FN} \tag{34}$$

3.5 Experimental Settings

All experiments were conducted using MATLAB R2024b on a machine equipped with i7-10750H CPU, 2.60GHz clock speed, and 32 GB RAM size. Each algorithm (WOA, EWOA, OWOA, mWOA, and HiWOA) follow their original configurations as described in their respective references. Each of them was executed independently for 30 runs to reduce stochastic bias. The dimension was the total feature size, whereas the population size was set to 30 solutions. The maximum number of iterations was fixed at 500 for all algorithms to ensure fair comparison.

The four filter-based FS methods described in Section 3.2 (ANOVA, Chi-square, Mutual Information, and Pearson Correlation Coefficient) were used individually as fitness functions to guide the search process. To evaluate the classification performance of the selected features, a kNN classifier was employed with k = 5, using 10-fold cross-validation to obtain reliable outcomes.

Based on the above experimental setup, the next section presents and discusses the results obtained for each algorithm × dataset × filter-based FS method combination, evaluated in terms of algorithmic stability, FS stability, and classification accuracy.

4. Results and Discussion

In this section, the performance of the proposed HiWOA is evaluated and compared against other WOA variants, namely standard WOA, EWOA, OWOA, and mWOA. The comparison is based on three main criteria: (1) algorithmic stability measured by the balance between exploration and exploitation, (2) FS stability measured by the modified Kuncheva Consistency Index, and (3) classification accuracy of the selected features using kNN classifier. All experiments were conducted on high-dimensional medical datasets, with each algorithm executed independently for 30 runs to reduce bias and ensure reliability of results.

4.1 Algorithmic Stability

Table 3 presents the exploration-exploitation ratio of all algorithms across five medical datasets under four different filter-based fitness functions, namely ANOVA, Chi-square, Mutual Information, and Pearson Correlation Coefficient.

For WOA, EWOA, and OWOA, the proportion of exploration remains very low, averaging between 5-10%, while exploitation dominates with more than 90% across all datasets. This imbalance indicates a strong tendency toward local search and probability of premature convergence, which may limit the ability to discover diverse feature subsets. In contrast, mWOA introduces a moderate improvement, achieving exploration levels of around 18-25%, which provides a more balanced search behavior compared to the standard WOA.

J. of Soft Computing and Data Mining Vol. 6 No. 3 (2025) p. 219-242

The proposed HiWOA consistently achieves the highest exploration rates across all filter functions and datasets, ranging from 28% to 37%. This improvement stems from two key modifications: the hierarchical leadership structure, which distributes guidance among three leaders (α, β, δ), and the arcsine-based control parameter, which enables a smoother shift from exploration toward exploitation.

Importantly, HiWOA demonstrates robustness across all filter-based fitness functions, with mean exploration consistently above 30% (ANOVA = 30.576%, Chi-square = 32.442%, Mutual Information = 33.171%, Pearson Correlation Coefficient = 33.917%). This indicates that the algorithm avoids being trapped in purely exploitative behavior, thereby enhancing the likelihood of reaching high-quality feature subsets while maintaining diversity in the search process.

In summary, the comparative results show that HiWOA offers a significantly more balanced exploration-exploitation ratio compared to both standard WOA and its variants, which is expected to contribute positively to consistency and classification performance in subsequent evaluations.

Table 3 *Algorithmic ratio (Exploration%: Exploitation%)*

FS	Datasets	WOA	EWOA	OWOA	mWOA	HiWOA
ANOVA	RNA-Seq	8.657: 91.343	11.784: 88.216	7.557: 92.443	23.333: 76.667	28.298: 71.702
	Lung	8.699: 91.301	8.628: 91.372	4.565: 95.435	24.225: 75.775	29.453: 70.547
	Lymphoma	7.386: 92.614	9.405: 90.595	4.816: 95.184	23.637: 76.363	31.383: 68.617
	SRBCT	9.851: 90.149	10.171: 89.829	5.876: 94.124	25.324: 74.676	31.134: 68.866
	Colon	7.515: 92.485	9.780: 90.220	7.207: 92.793	26.231: 73.769	32.614: 67.386
	Mean	8.422: 91.578	9.954: 90.046	6.004: 93.996	24.550: 75.450	30.576: 69.424
Chi-square	RNA-Seq	4.431: 95.569	7.929: 92.071	3.538: 96.462	14.304: 85.696	30.526: 69.474
	Lung	6.643: 93.357	8.541: 91.459	6.125: 93.875	24.723: 75.277	35.758: 64.242
	Lymphoma	5.951: 94.049	9.657: 90.343	4.673: 95.327	15.750: 84.250	32.930: 67.070
	SRBCT	3.655: 96.345	8.725: 91.275	3.548: 96.452	17.171: 82.829	33.099: 66.901
	Colon	14.555: 85.445	26.956: 73.044	13.919: 86.081	28.577: 71.423	29.898: 70.102
	Mean	7.047: 92.953	12.362: 87.638	6.361: 93.639	20.105: 79.895	32.442: 67.558
Mutual Information	RNA-Seq	4.338: 95.662	11.505: 88.495	3.652: 96.348	15.404: 84.596	33.049: 66.951
	Lung	7.205: 92.795	9.412: 90.588	7.674: 92.326	21.594: 78.406	31.325: 68.675
	Lymphoma	5.271: 94.729	10.372: 89.628	4.720: 95.280	15.874: 84.126	32.566: 67.434
	SRBCT	7.613: 92.387	8.831: 91.169	4.766: 95.234	16.985: 83.015	33.874: 66.126
	Colon	5.440: 94.560	6.638: 93.362	4.654: 95.346	21.224: 78.776	35.043: 64.957
	Mean	5.973: 94.027	9.352: 90.648	5.093: 94.907	18.216: 81.784	33.171: 66.829
Pearson Correlation Coefficient	RNA-Seq	6.792: 93.208	7.567: 92.433	6.788: 93.212	12.288: 87.712	33.639: 66.361
	Lung	3.964: 96.036	7.486: 92.514	5.827: 94.173	16.081: 83.919	32.253: 67.747
	Lymphoma	7.167: 92.833	8.806: 91.194	4.314: 95.686	14.907: 85.093	32.986: 67.014
	SRBCT	6.862: 93.138	7.525: 92.475	3.759: 96.241	20.875: 79.125	33.690: 66.310
	Colon	5.342: 94.658	11.277: 88.723	6.174: 93.826	21.277: 78.723	37.018: 62.982
	Mean	6.025: 93.975	8.532: 91.468	5.372: 94.628	17.086: 82.914	33.917: 66.083
Overall Performance		6.867: 43.133	10.050: 39.950	5.708: 44.292	19.989: 30.011	32.527: 17.473

To simplify the comparison, the Algorithmic Gap was introduced, defined as the absolute difference between the two phases, i.e., $|Exploration\% - Exploitation\%|$. A smaller gap indicates a closer alignment between exploration and exploitation, whereas larger gaps suggest an imbalance in the search dynamics. The detailed results of all WOA variants under different filter-based FS methods are summarized in Table 4.

Table 4 *Algorithmic gap (Exploration%-Exploitation%)*

FS	Datasets	WOA	EWOA	OWOA	mWOA	HiWOA
ANOVA	RNA-Seq	82.686	76.432	84.886	53.334	43.404
	Lung	82.602	82.744	90.870	51.550	41.094
	Lymphoma	85.228	81.190	90.368	52.726	37.234
	SRBCT	80.298	79.658	88.248	49.352	37.732
	Colon	84.970	80.440	85.586	47.538	34.772
	Mean	83.156	80.092	87.992	50.900	38.848
Chi-square	RNA-Seq	91.138	84.142	92.924	71.392	38.948
	Lung	86.714	82.918	87.750	50.554	28.484
	Lymphoma	88.098	80.686	90.654	68.500	34.140
	SRBCT	92.690	82.550	92.904	65.658	33.802
	Colon	70.890	46.088	72.162	42.846	40.204
	Mean	85.906	75.276	87.278	59.790	35.116
Mutual Information	RNA-Seq	91.324	76.990	92.696	69.192	33.902
	Lung	85.590	81.176	84.652	56.812	37.350
	Lymphoma	89.458	79.256	90.560	68.252	34.868
	SRBCT	84.774	82.338	90.468	66.030	32.252
	Colon	89.120	86.724	90.692	57.552	29.914
	Mean	88.054	81.296	89.814	63.568	33.658
Pearson Correlation Coefficient	RNA-Seq	86.416	84.866	86.424	75.424	32.722
	Lung	92.072	85.028	88.346	67.838	35.494
	Lymphoma	85.666	82.388	91.372	70.186	34.028
	SRBCT	86.276	84.950	92.482	58.250	32.620
	Colon	89.316	77.446	87.652	57.446	25.964
	Mean	87.950	82.936	89.256	65.828	32.166
Overall Performance		86.266	79.900	88.585	60.022	34.947

Based on Table 4, the results clearly show that WOA, EWOA, and OWOA exhibit very large gaps, typically around 80% and 90%, reflecting a strong dominance of exploitation over exploration. Notably, mWOA achieves moderate improvements, reducing the gap to around 50-70%, yet it still shows limited ability to maintain high exploration. By contrast, HiWOA achieves the smallest gaps across all datasets and filters, ranging between 25.964% and 43.404%. On average, HiWOA records gaps of 32-39%, representing a reduction of nearly 50% compared to standard WOA. The best case is observed on the Colon dataset with Pearson Correlation Coefficient, where HiWOA attains the lowest gap of 25.964%, indicating a more-balanced search behavior.

Fig. 5 presents the exploration-exploitation gap of HiWOA across different filter-based FS methods (refer to the last column of Table 4). Among the filter-based methods, Pearson Correlation Coefficient has the smallest algorithmic gap in most datasets, except for Lung. In contrast, ANOVA produces the largest gap in all datasets except for Colon. Overall, the order of algorithmic gaps from biggest to smallest is ANOVA > Chi-square > Mutual Information > Pearson Correlation Coefficient.

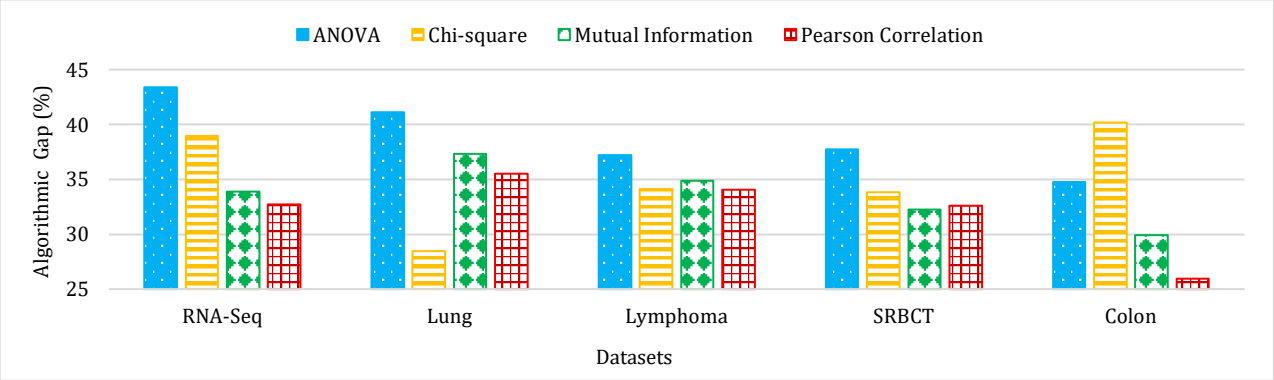

Fig. 5 *Algorithmic gap (%) using different filter-based FS methods on all datasets by HiWOA*

Furthermore, Fig. 6 to Fig. 9 illustrate the exploration-exploitation ratio across iterations for the RNA-Seq dataset under four different filter-based fitness functions: ANOVA (Fig. 6), Chi-square (Fig. 7), Mutual Information (Fig. 8), and Pearson Correlation Coefficient (Fig. 9). Each figure compares the behavior of five algorithms: WOA,

J. of Soft Computing and Data Mining Vol. 6 No. 3 (2025) p. 219-242

EWOA, OWOA, mWOA, and the proposed HiWOA. Across all filter functions, a consistent pattern is observed: WOA, EWOA, and OWOA converge rapidly into exploitation with very limited exploration, while mWOA achieves moderate balance. HiWOA demonstrates the most stable trade-off, maintaining exploration at approximately 30% while gradually increasing exploitation, confirming the numerical trends reported in Table 3 and Table 4.

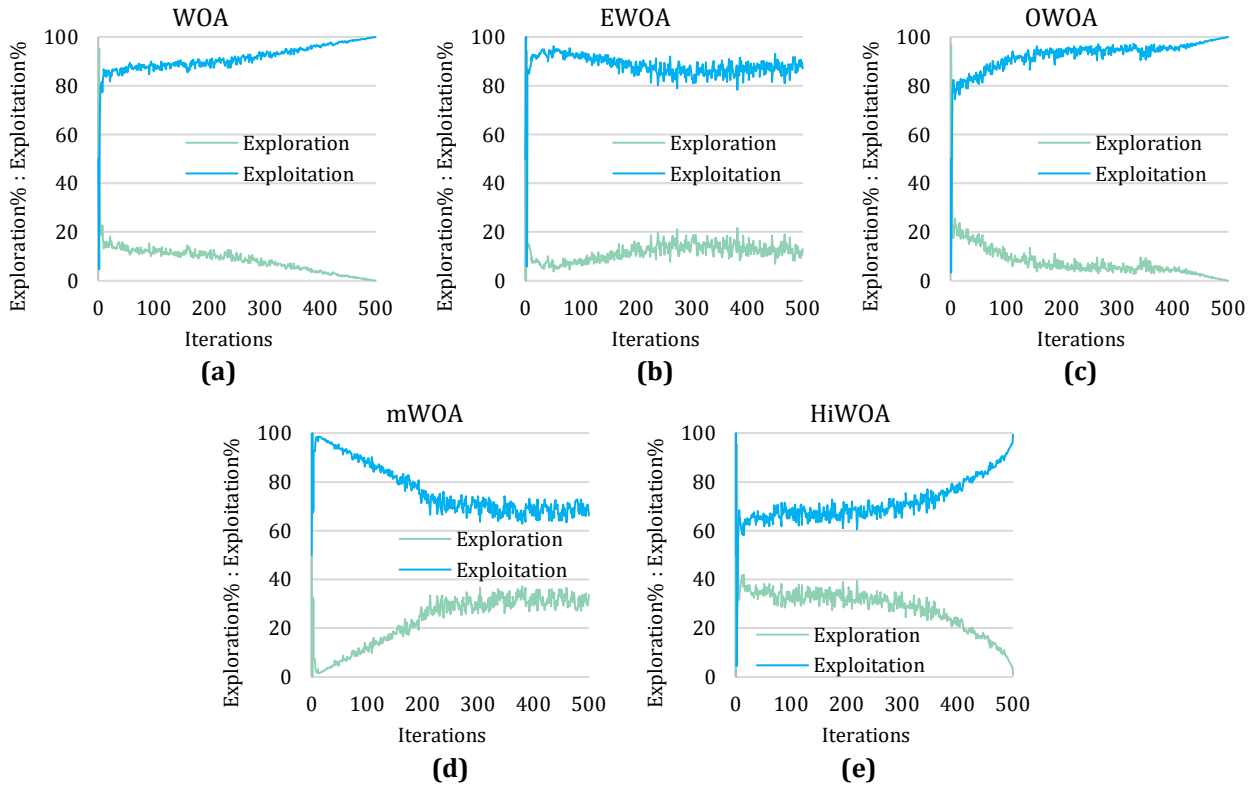

Fig. 6 *Exploration%: Exploitation% ratio for dataset RNA-Seq using ANOVA FS method (a) WOA; (b) EWOA; (c) OWOA; (d) mWOA; (e) HiWOA*

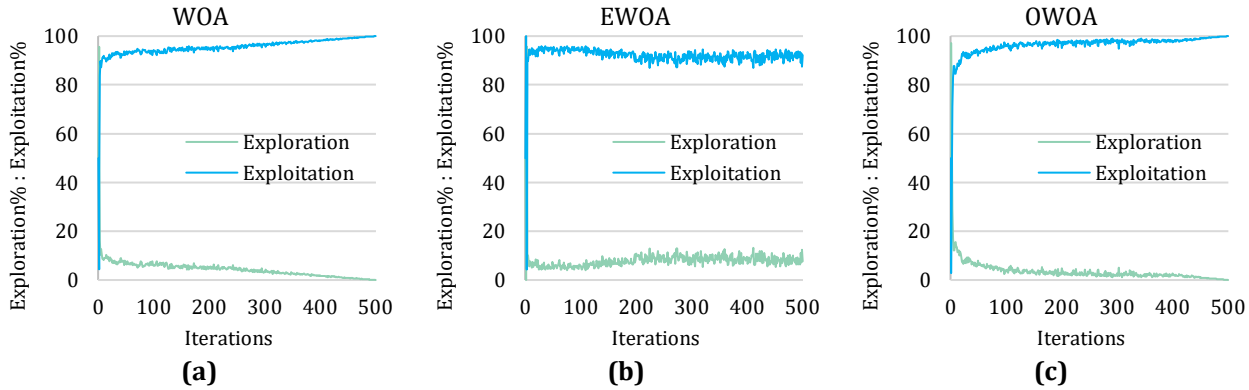

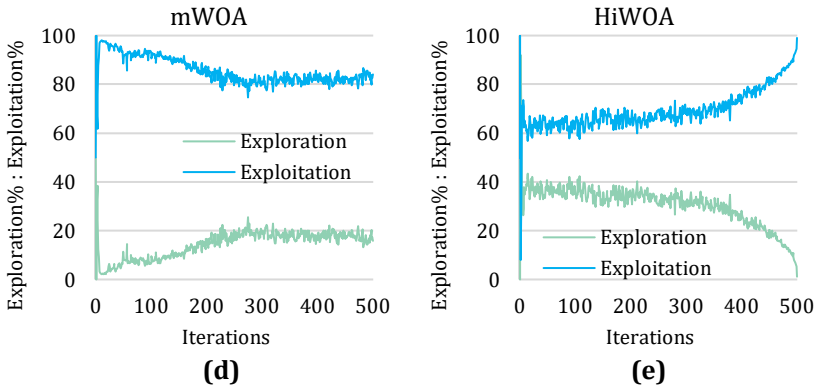

Fig. 7 *Exploration%: Exploitation% ratio for dataset RNA-Seq using Chi-square FS method (a) WOA; (b) EWOA; (c) OWOA; (d) mWOA; (e) HiWOA*

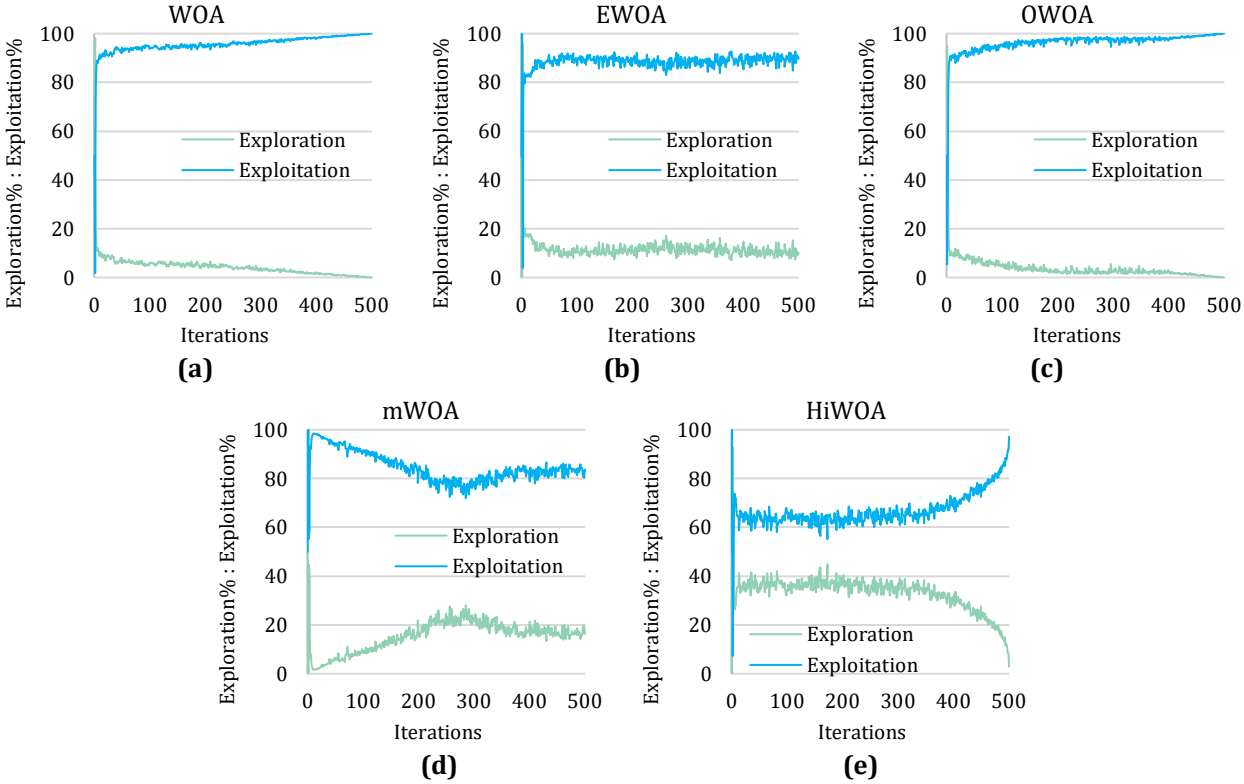

Fig. 8 *Exploration%: Exploitation% ratio for dataset RNA-Seq using Mutual Information FS method (a) WOA; (b) EWOA; (c) OWOA; (d) mWOA; (e) HiWOA*

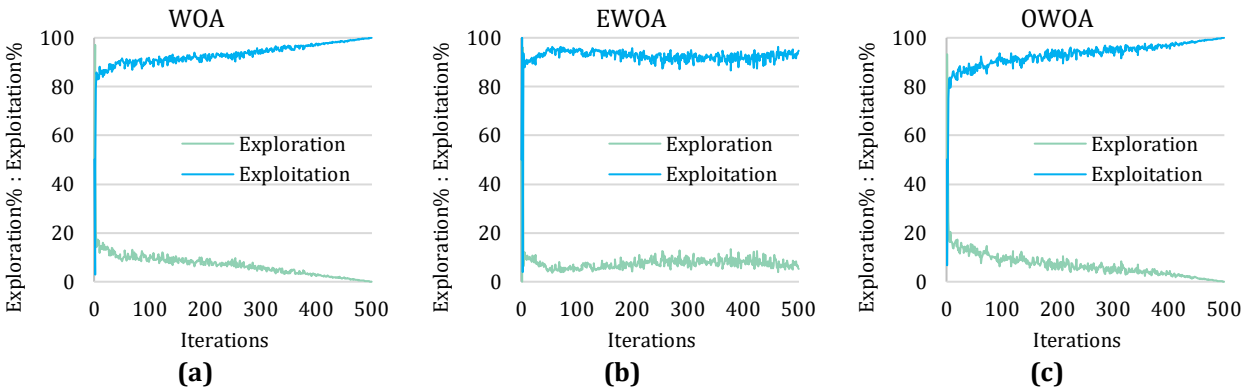

J. of Soft Computing and Data Mining Vol. 6 No. 3 (2025) p. 219-242

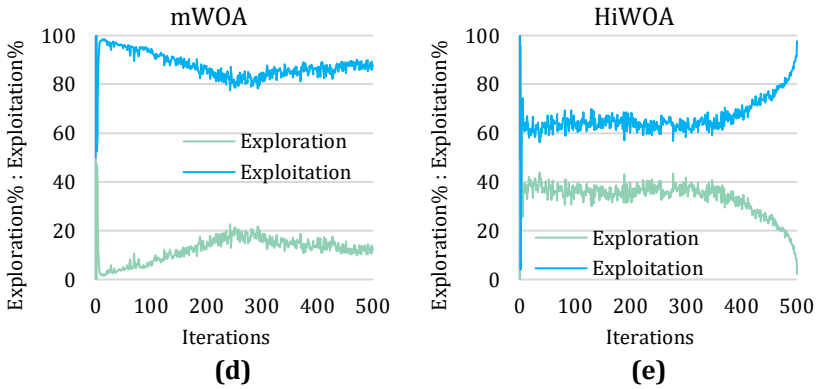

Fig. 9 *Exploration%: Exploitation% ratio for dataset RNA-Seq using Pearson Correlation Coefficient FS method (a) WOA; (b) EWOA; (c) OWOA; (d) mWOA; (e) HiWOA*

As shown in Fig. 6 to Fig. 9, although minor fluctuations exist depending on the filter, the overall dynamics remain similar, with HiWOA being the most algorithmic balanced. These findings demonstrate that the hierarchical leadership and arcsine-based control in HiWOA effectively reduce the imbalance between exploration and exploitation seen in standard WOA variants. By maintaining a more balanced search behavior, HiWOA enhances the FS stability and yields improved classification performance.

4.2 Feature Selection Stability

FS stability is a critical criterion in high-dimensional biomedical datasets, since unstable algorithms may produce very different subsets across repeated runs, limiting their interpretability and reliability. To quantify stability, the MKCI was adopted. This index measures the average pairwise overlap between feature subsets obtained from multiple runs of the same algorithm.

In this study, each algorithm was executed 30 independent times on every dataset for each filter-based fitness function. The MKCI was then computed as the average of all pairwise comparisons among the 30 subsets, resulting in 435 pairwise values per case, as $C(30,2) = 435$. For example, the detailed calculation of MKCI when selecting features from the SRBCT dataset via HiWOA using Pearson Correlation Coefficient is provided in Appendix A. The final MKCI values for all algorithms and datasets are reported in Table 5.

Table 5 *FS consistency index computed by MKCI*

FS	Datasets	WOA	EWOA	OWOA	mWOA	HiWOA
ANOVA	RNA-Seq	0.00230	0.00185	0.00259	0.00259	0.00312
	Lung	0.00240	0.00152	0.00276	0.00253	0.00359
	Lymphoma	0.00406	0.00419	0.00410	0.00477	0.00781
	SRBCT	0.00619	0.00455	0.00510	0.00751	0.01046
	Colon	0.00636	0.00492	0.00602	0.00672	0.00950
	Mean	0.00426	0.00341	0.00411	0.00482	0.00690
Chi-square	RNA-Seq	0.00088	0.00019	0.00134	0.00092	0.00264
	Lung	0.00139	0.00040	0.00134	0.00213	0.00363
	Lymphoma	0.00372	0.00143	0.00299	0.00282	0.00643
	SRBCT	0.00381	0.00155	0.00359	0.00412	0.00904
	Colon	0.01450	0.01093	0.00984	0.01022	0.01400
	Mean	0.00486	0.00290	0.00382	0.00404	0.00715
Mutual Information	RNA-Seq	0.00139	0.00042	0.00133	0.00098	0.00245
	Lung	0.00221	0.00081	0.00230	0.00184	0.00370
	Lymphoma	0.00340	0.00196	0.00292	0.00265	0.00626
	SRBCT	0.00509	0.00285	0.00368	0.00363	0.01069
	Colon	0.00445	0.00175	0.00462	0.00300	0.00776
	Mean	0.00331	0.00156	0.00297	0.00242	0.00617
Pearson correlation coefficient	RNA-Seq	0.00119	0.00010	0.00091	0.00028	0.00260
	Lung	0.00156	0.00041	0.00158	0.00112	0.00343
	Lymphoma	0.00347	0.00126	0.00350	0.00318	0.00604
	SRBCT	0.00496	0.00319	0.00442	0.00333	0.00769
	Colon	0.00460	0.00414	0.00622	0.00583	0.00935
	Mean	0.00316	0.00182	0.00332	0.00275	0.00582
Overall Performance		0.00390	0.00242	0.00356	0.00351	0.00651

The results in Table 5 demonstrate that HiWOA achieves the highest MKCI scores across all datasets and filter methods, indicating superior stability in FS. For example, in the SRBCT dataset, HiWOA reached MKCI values of 0.01046 (ANOVA), 0.00904 (Chi-square), 0.01069 (Mutual Information), and 0.00769 (Pearson Correlation Coefficient), all of which are higher than competing algorithms. Similarly, in the Lung and Colon datasets, HiWOA maintained higher MKCI values than WOA, EWOA, OWOA, and mWOA under every filter-based method. When averaged across all datasets, HiWOA consistently outperformed the other algorithms with mean MKCI values of 0.00690 (ANOVA), 0.00715 (Chi-square), 0.00617 (Mutual Information), and 0.00582 (Pearson Correlation Coefficient). In contrast, WOA and EWOA frequently produced lower stability scores, in some cases approaching zero (e.g., Pearson Correlation Coefficient on RNA-Seq with EWOA = 0.00010).

Fig. 10 illustrates the consistency index of HiWOA across different datasets and filter-based FS methods. The results show that stability levels vary depending on both the dataset and the filter-based FS methods. For larger datasets such as RNA-Seq and Lung, the MKCI values remain relatively low (≈0.002-0.004), indicating lower consistency in selecting similar features across 30 runs. In contrast, for smaller datasets (though still high-dimensional) like SRBCT and Colon, HiWOA achieves markedly higher stability, with MKCI values exceeding 0.010 for ANOVA, Mutual Information, and Chi-square FS methods. Notably, the Colon dataset under Chi-square selection yields the highest stability value (0.014), suggesting a strong overlap in features across repeated runs.

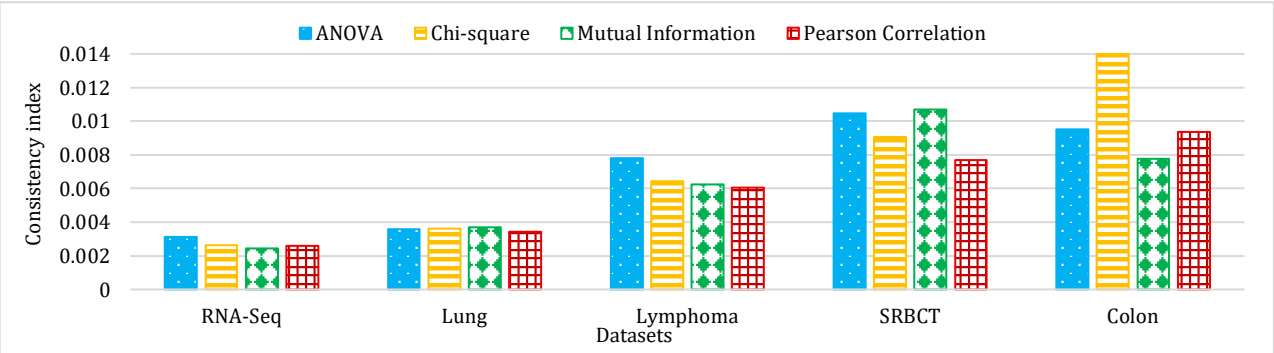

Fig. 10 *Consistency index using different filter-based FS methods on all datasets by HiWOA*

Among the filter-based methods, the ranking of average FS stability from highest to lowest is Chi-square > ANOVA > Mutual Information > Pearson Correlation Coefficient. Overall, the results of FS stability suggest that HiWOA can produce more stable feature subsets compared to the other WOA variants, which is particularly desirable in medical datasets where reliability is important.

J. of Soft Computing and Data Mining Vol. 6 No. 3 (2025) p. 219-242

4.3 Classification Accuracy

To assess the discriminative quality of the selected features, the subsets generated by each algorithm were evaluated using a kNN classifier. Table 6 summarizes the classification accuracies obtained across all datasets and filter-based FS methods.

Table 6 *Classification accuracy obtained by kNN (%)*

FS	Datasets	WOA	EWOA	OWOA	mWOA	HiWOA
ANOVA	RNA-Seq	100.000	99.563	100.000	100.000	100.000
	Lung	87.000	82.250	84.750	92.250	93.000
	Lymphoma	96.667	84.444	96.667	90.000	100.000
	SRBCT	80.625	80.625	90.625	96.250	100.000
	Colon	86.667	86.667	84.167	90.000	96.667
	Mean	90.192	86.710	91.242	93.700	97.933
Chi-square	RNA-Seq	99.875	98.688	99.750	99.875	100.000
	Lung	90.250	95.250	86.750	95.500	97.250
	Lymphoma	76.667	87.778	91.111	88.889	96.667
	SRBCT	73.125	76.250	75.625	85.625	98.750
	Colon	90.833	89.167	85.833	85.000	94.167
	Mean	86.150	89.426	87.814	90.978	97.367
Mutual Information	RNA-Seq	99.000	99.625	99.063	100.000	100.000
	Lung	83.000	85.250	87.750	89.250	95.500
	Lymphoma	82.222	70.000	86.667	80.000	100.000
	SRBCT	80.000	73.125	66.875	73.750	90.625
	Colon	79.167	64.167	74.167	93.333	91.667
	Mean	84.678	78.433	82.904	87.267	95.558
Pearson correlation coefficient	RNA-Seq	99.938	99.000	100.000	99.938	100.000
	Lung	84.250	84.750	87.500	84.500	95.000
	Lymphoma	86.667	92.222	80.000	94.444	95.556
	SRBCT	59.375	50.625	73.750	68.750	94.375
	Colon	69.167	75.000	74.167	82.500	90.833
	Mean	79.879	80.319	83.083	86.026	95.153
Overall Performance		85.225	83.722	86.261	89.493	96.503

Across all filter-based FS methods, the proposed HiWOA consistently achieves the highest classification accuracy, outperforming standard WOA and its variants. On average, HiWOA records accuracies of 97.933% (ANOVA), 97.367% (Chi-square), 95.558% (Mutual Information), and 95.153% (Pearson Correlation Coefficient), clearly surpassing the competing methods. On the contrary, WOA and EWOA often exhibit lower accuracy, particularly in smaller datasets such as SRBCT and Colon.

Dataset-specific observations further reinforce the superiority of HiWOA. For instance, in the Lymphoma dataset, HiWOA achieves 100% accuracy across both ANOVA and Mutual Information, while other algorithms range between 70.000-96.667%. Similarly, for the SRBCT dataset, HiWOA obtains 100% (ANOVA) and 98.75% (Chi-square), whereas the best performance among the other variants is 96.25% (mWOA with ANOVA). In the Colon dataset, HiWOA secures higher accuracies (up to 96.667% with ANOVA) compared to the competing methods.

When comparing the FS methods, ANOVA and Chi-square generally yield the strongest classification outcomes across all algorithms, followed by Mutual Information, while Pearson correlation shows relatively lower performance in most cases. Nonetheless, HiWOA maintains high accuracy even under Pearson Correlation Coefficient (up to 95.556% in Lymphoma), further demonstrating its robustness.

Fig. 11 presents the classification accuracy of HiWOA across all datasets using different filter-based FS methods. The results show that HiWOA achieves the highest accuracy on RNA-Seq and strong results for all other datasets. Among the filter-based FS methods, the overall classification accuracy of HiWOA follows the order: ANOVA > Chi-square > Mutual Information > Pearson correlation.

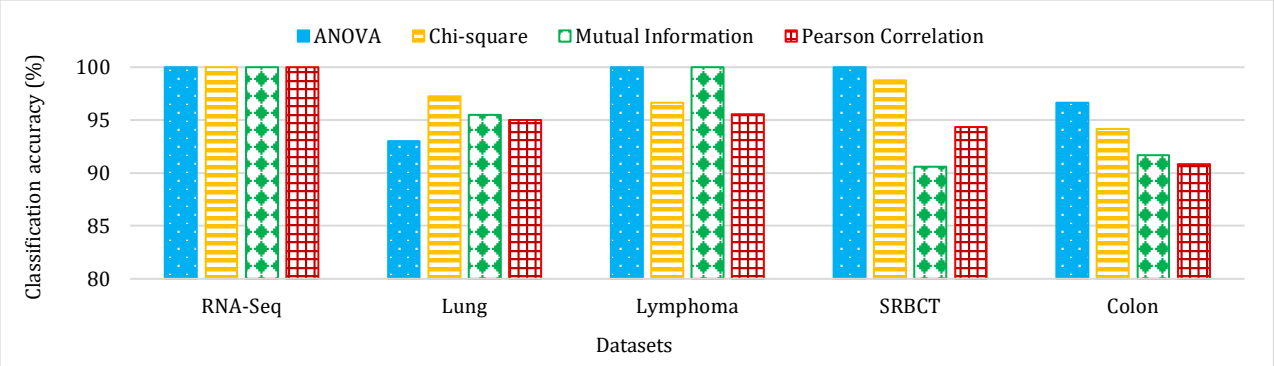

Fig. 11 *Classification accuracy (%) using different filter-based FS methods on all datasets by HiWOA*

In summary, the experimental results from sub-sections algorithmic stability, FS stability, and classification accuracy collectively show that HiWOA outperforms standard WOA and its variants in the context of filter-based FS for high-dimensional medical datasets. In terms of algorithmic stability, HiWOA achieved the most balanced trade-off between exploration and exploitation, while maintaining diversity (high exploration%). Stability analysis further confirmed that HiWOA generated more consistent feature subsets across multiple runs, as indicated by higher MKCI values. Finally, classification performance using kNN validated the quality of the selected features, with HiWOA delivering the highest accuracy across all datasets and filter-based FS methods. Among them, ANOVA method emerged as the most effective method, as it produced features that contributed into the strongest classification results, confirming their higher discriminative quality in evaluating the fitness of features. Therefore, these findings establish HiWOA combined with ANOVA filter-based FS as the most robust and reliable framework for handling high-dimensional medical data, since this combination produced the highest classification accuracy while maintaining acceptable algorithmic balance and FS stability across all datasets.

4.4 Conclusion

This paper presented a Hierarchical Whale Optimization Algorithm (HiWOA) for filter-based FS in high-dimensional medical datasets. Unlike standard WOA and its existing variants, HiWOA incorporates a hierarchical leadership mechanism and an arcsine-based control parameter to improve the balance between exploration and exploitation. While earlier studies applied HiWOA mainly to optimization or wrapper-based FS problems, this work is the first to extend it to purely filter-based FS.

The experiments were structured by evaluating four widely used filter-based methods (ANOVA, Chi-square, Mutual Information, and Pearson Correlation Coefficient) on multiple benchmark medical datasets. Each WOA variant was executed 30 independent times to ensure statistical reliability, with performance assessed in terms of algorithmic stability, FS stability, and classification accuracy using kNN.

The results clearly demonstrate the benefits of HiWOA over standard WOA and its variants. HiWOA achieved a more balanced search dynamic, produced feature subsets with higher consistency across runs, and delivered superior classification performance. Among the filter-based methods used, ANOVA proved to be the most effective, consistently yielding features of higher discriminative quality. Thus, the combination of HiWOA with ANOVA-based FS emerges as a strong and reliable approach for analyzing high-dimensional medical datasets.

Since this study is limited to a small set of benchmark datasets, a single classifier, and filter-based FS, future work may address these limitations by testing HiWOA with diverse biomedical data, integrating other classifiers including deep learning models, and exploring hybrid FS strategies to further assess its generalizability.

Acknowledgement

This research was supported by Ministry of Higher Education (MOHE) through Fundamental Research Grant Scheme (FRGS/1/2023/ICT02/UTHM/02/6).

Conflict of Interest

Authors declare that there is no conflict of interests regarding the publication of the paper.

J. of Soft Computing and Data Mining Vol. 6 No. 3 (2025) p. 219-242

Author Contribution

The authors confirm contribution to the paper as follows: ***study conception and design:*** *Li Yu Yab, Noorhaniza Wahid, Rahayu A Hamid;* ***data collection:*** *Li Yu Yab;* ***analysis and interpretation of results:*** *Li Yu Yab;* ***draft manuscript preparation:*** *Li Yu Yab, Noorhaniza Wahid, Rahayu A Hamid, José Machado. All authors reviewed the results and approved the final version of the manuscript.*

Appendix A: Pairwise MKCI calculation

Table A1 *Detailed MKCI values from 30 independent runs of HiWOA on the SRBCT dataset, where feature relevance was evaluated using Pearson Correlation Coefficient as the filter-based fitness function.*

Pair	E_1	E_2	r	n	k_1	k_2	MKCI	Pair	E_1	E_2	r	n	k_1	k_2	MKCI
1	1	2	4	2308	883	14	0.00155	51	2	24	0	2308	14	37	0.00000
2	1	3	32	2308	883	103	0.00878	52	2	25	1	2308	14	138	0.00119
3	1	4	252	2308	883	600	0.03436	53	2	26	5	2308	14	449	0.00510
4	1	5	33	2308	883	99	0.00577	54	2	27	0	2308	14	42	0.00000
5	1	6	92	2308	883	211	0.01405	55	2	28	0	2308	14	87	0.00000
6	1	7	4	2308	883	7	0.00150	56	2	29	2	2308	14	374	0.00072
7	1	8	14	2308	883	32	0.00202	57	2	30	1	2308	14	156	0.00035
8	1	9	40	2308	883	95	0.00432	58	3	4	24	2308	103	600	0.00484
9	1	10	33	2308	883	90	0.00169	59	3	5	3	2308	103	99	0.01439
10	1	11	210	2308	883	579	0.01741	60	3	6	11	2308	103	211	0.00786
11	1	12	43	2308	883	106	0.00290	61	3	7	0	2308	103	7	0.00000
12	1	13	22	2308	883	71	0.00603	62	3	8	3	2308	103	32	0.01548
13	1	14	52	2308	883	130	0.00272	63	3	9	2	2308	103	95	0.02268
14	1	15	23	2308	883	56	0.00183	64	3	10	5	2308	103	90	0.00994
15	1	16	11	2308	883	25	0.00164	65	3	11	20	2308	103	579	0.01056
16	1	17	131	2308	883	328	0.00728	66	3	12	5	2308	103	106	0.00266
17	1	18	426	2308	883	1050	0.03747	67	3	13	6	2308	103	71	0.02836
18	1	19	100	2308	883	295	0.01670	68	3	14	8	2308	103	130	0.01770
19	1	20	101	2308	883	277	0.00640	69	3	15	4	2308	103	56	0.01493
20	1	21	29	2308	883	81	0.00233	70	3	16	1	2308	103	25	0.00114
21	1	22	179	2308	883	472	0.00225	71	3	17	15	2308	103	328	0.00116
22	1	23	32	2308	883	76	0.00342	72	3	18	54	2308	103	1050	0.00712
23	1	24	16	2308	883	37	0.00212	73	3	19	14	2308	103	295	0.00296
24	1	25	48	2308	883	138	0.00578	74	3	20	23	2308	103	277	0.04020
25	1	26	167	2308	883	449	0.00672	75	3	21	3	2308	103	81	0.00619
26	1	27	13	2308	883	42	0.00354	76	3	22	16	2308	103	472	0.01123
27	1	28	34	2308	883	87	0.00084	77	3	23	3	2308	103	76	0.00393
28	1	29	142	2308	883	374	0.00147	78	3	24	1	2308	103	37	0.00643
29	1	30	54	2308	883	156	0.00690	79	3	25	6	2308	103	138	0.00120
30	2	3	1	2308	14	103	0.00367	80	3	26	22	2308	103	449	0.00457
31	2	4	3	2308	14	600	0.00107	81	3	27	3	2308	103	42	0.01113
32	2	5	2	2308	14	99	0.01422	82	3	28	3	2308	103	87	0.00890
33	2	6	3	2308	14	211	0.00820	83	3	29	18	2308	103	374	0.00366
34	2	7	0	2308	14	7	0.00000	84	3	30	8	2308	103	156	0.00697
35	2	8	1	2308	14	32	0.02534	85	4	5	28	2308	600	99	0.00394
36	2	9	0	2308	14	95	0.00000	86	4	6	55	2308	600	211	0.00027
37	2	10	0	2308	14	90	0.00000	87	4	7	2	2308	600	7	0.00030
38	2	11	5	2308	14	579	0.00259	88	4	8	8	2308	600	32	0.00054
39	2	12	0	2308	14	106	0.00000	89	4	9	27	2308	600	95	0.00400
40	2	13	0	2308	14	71	0.00000	90	4	10	18	2308	600	90	0.00936
41	2	14	1	2308	14	130	0.00164	91	4	11	165	2308	600	579	0.03222
42	2	15	0	2308	14	56	0.00000	92	4	12	22	2308	600	106	0.00971
43	2	16	0	2308	14	25	0.00000	93	4	13	21	2308	600	71	0.00437
44	2	17	2	2308	14	328	0.00003	94	4	14	38	2308	600	130	0.00743
45	2	18	6	2308	14	1050	0.00035	95	4	15	22	2308	600	56	0.01271
46	2	19	4	2308	14	295	0.00754	96	4	16	8	2308	600	25	0.00253
47	2	20	2	2308	14	277	0.00116	97	4	17	88	2308	600	328	0.00531
48	2	21	0	2308	14	81	0.00000	98	4	18	273	2308	600	1050	0.00005
49	2	22	4	2308	14	472	0.00242	99	4	19	69	2308	600	295	0.01469
50	2	23	0	2308	14	76	0.00000	100	4	20	67	2308	600	277	0.00949

Note: Pair=Pair counter; E_1=First experiment ID; E_2=Second experiment ID; r=Number of overlapped features; n=Number of all features in the dataset; k_1=Number of selected features in the first experiment; k_2=Number of selected features in the second experiment; MKCI= computed pairwise consistency index

Table A1 *(continued).*

Pair	E_1	E_2	r	n	k_1	k_2	MKCI	Pair	E_1	E_2	r	n	k_1	k_2	MKCI
101	4	21	20	2308	600	81	0.00183	171	7	19	0	2308	7	295	0.00000
102	4	22	118	2308	600	472	0.00985	172	7	20	2	2308	7	277	0.00420
103	4	23	20	2308	600	76	0.00042	173	7	21	0	2308	7	81	0.00000
104	4	24	11	2308	600	37	0.00234	174	7	22	2	2308	7	472	0.00121
105	4	25	36	2308	600	138	0.00022	175	7	23	0	2308	7	76	0.00000
106	4	26	116	2308	600	449	0.00150	176	7	24	0	2308	7	37	0.00000
107	4	27	16	2308	600	42	0.00863	177	7	25	1	2308	7	138	0.00423
108	4	28	23	2308	600	87	0.00066	178	7	26	0	2308	7	449	0.00000
109	4	29	103	2308	600	374	0.01148	179	7	27	0	2308	7	42	0.00000
110	4	30	45	2308	600	156	0.00795	180	7	28	0	2308	7	87	0.00000
111	5	6	2	2308	99	211	0.03491	181	7	29	1	2308	7	374	0.00036
112	5	7	0	2308	99	7	0.00000	182	7	30	1	2308	7	156	0.00339
113	5	8	2	2308	99	32	0.00643	183	8	9	1	2308	32	95	0.00339
114	5	9	1	2308	99	95	0.03239	184	8	10	3	2308	32	90	0.01974
115	5	10	4	2308	99	90	0.00147	185	8	11	11	2308	32	579	0.00521
116	5	11	26	2308	99	579	0.00210	186	8	12	1	2308	32	106	0.00449
117	5	12	2	2308	99	106	0.02510	187	8	13	0	2308	32	71	0.00000
118	5	13	5	2308	99	71	0.02037	188	8	14	3	2308	32	130	0.00934
119	5	14	8	2308	99	130	0.01948	189	8	15	0	2308	32	56	0.00000
120	5	15	5	2308	99	56	0.02689	190	8	16	1	2308	32	25	0.02064
121	5	16	1	2308	99	25	0.00074	191	8	17	8	2308	32	328	0.01067
122	5	17	5	2308	99	328	0.02889	192	8	18	22	2308	32	1050	0.00719
123	5	18	37	2308	99	1050	0.00800	193	8	19	7	2308	32	295	0.01000
124	5	19	13	2308	99	295	0.00123	194	8	20	7	2308	32	277	0.01157
125	5	20	14	2308	99	277	0.00799	195	8	21	1	2308	32	81	0.00154
126	5	21	4	2308	99	81	0.00550	196	8	22	7	2308	32	472	0.00098
127	5	22	24	2308	99	472	0.00831	197	8	23	0	2308	32	76	0.00000
128	5	23	4	2308	99	76	0.00773	198	8	24	1	2308	32	37	0.01335
129	5	24	3	2308	99	37	0.01450	199	8	25	1	2308	32	138	0.00671
130	5	25	9	2308	99	138	0.02332	200	8	26	11	2308	32	449	0.01078
131	5	26	22	2308	99	449	0.00638	201	8	27	0	2308	32	42	0.00000
132	5	27	3	2308	99	42	0.01233	202	8	28	3	2308	32	87	0.02091
133	5	28	2	2308	99	87	0.01818	203	8	29	11	2308	32	374	0.01577
134	5	29	19	2308	99	374	0.00826	204	8	30	3	2308	32	156	0.00544
135	5	30	7	2308	99	156	0.00207	205	9	10	6	2308	95	90	0.02514
136	6	7	1	2308	211	7	0.00171	206	9	11	26	2308	95	579	0.00390
137	6	8	2	2308	211	32	0.00445	207	9	12	9	2308	95	106	0.04562
138	6	9	9	2308	211	95	0.00156	208	9	13	3	2308	95	71	0.00084
139	6	10	8	2308	211	90	0.00112	209	9	14	4	2308	95	130	0.01084
140	6	11	58	2308	211	579	0.00963	210	9	15	2	2308	95	56	0.00329
141	6	12	10	2308	211	106	0.00154	211	9	16	1	2308	95	25	0.00031
142	6	13	7	2308	211	71	0.00249	212	9	17	12	2308	95	328	0.00477
143	6	14	6	2308	211	130	0.02955	213	9	18	39	2308	95	1050	0.00419
144	6	15	3	2308	211	56	0.01030	214	9	19	8	2308	95	295	0.01465
145	6	16	3	2308	211	25	0.00342	215	9	20	8	2308	95	277	0.01281
146	6	17	33	2308	211	328	0.01011	216	9	21	3	2308	95	81	0.00364
147	6	18	89	2308	211	1050	0.00733	217	9	22	23	2308	95	472	0.00789
148	6	19	28	2308	211	295	0.00385	218	9	23	2	2308	95	76	0.01228
149	6	20	26	2308	211	277	0.00269	219	9	24	2	2308	95	37	0.00510
150	6	21	6	2308	211	81	0.00690	220	9	25	5	2308	95	138	0.00514
151	6	22	55	2308	211	472	0.02763	221	9	26	16	2308	95	449	0.00576
152	6	23	9	2308	211	76	0.01006	222	9	27	3	2308	95	42	0.01363
153	6	24	2	2308	211	37	0.00666	223	9	28	7	2308	95	87	0.03740
154	6	25	10	2308	211	138	0.01319	224	9	29	13	2308	95	374	0.00668
155	6	26	33	2308	211	449	0.01973	225	9	30	9	2308	95	156	0.01724
156	6	27	6	2308	211	42	0.01043	226	10	11	25	2308	90	579	0.00435
157	6	28	5	2308	211	87	0.01455	227	10	12	3	2308	90	106	0.01113
158	6	29	34	2308	211	374	0.00056	228	10	13	1	2308	90	71	0.02028
159	6	30	15	2308	211	156	0.00375	229	10	14	9	2308	90	130	0.03146
160	7	8	0	2308	7	32	0.00000	230	10	15	2	2308	90	56	0.00209
161	7	9	0	2308	7	95	0.00000	231	10	16	0	2308	90	25	0.00000
162	7	10	0	2308	7	90	0.00000	232	10	17	11	2308	90	328	0.00568
163	7	11	1	2308	7	579	0.00131	233	10	18	48	2308	90	1050	0.00699
164	7	12	0	2308	7	106	0.00000	234	10	19	10	2308	90	295	0.00530
165	7	13	0	2308	7	71	0.00000	235	10	20	12	2308	90	277	0.00450
166	7	14	1	2308	7	130	0.00467	236	10	21	2	2308	90	81	0.01334
167	7	15	0	2308	7	56	0.00000	237	10	22	15	2308	90	472	0.00751
168	7	16	0	2308	7	25	0.00000	238	10	23	3	2308	90	76	0.00042
169	7	17	2	2308	7	328	0.00307	239	10	24	1	2308	90	37	0.00500
170	7	18	2	2308	7	1050	0.00113	240	10	25	8	2308	90	138	0.01975

J. of Soft Computing and Data Mining Vol. 6 No. 3 (2025) p. 219-242

Table A1 *(continued).*

Pair	E_1	E_2	r	n	k_1	k_2	MKCI	Pair	E_1	E_2	r	n	k_1	k_2	MKCI
241	10	26	18	2308	90	449	0.00114	311	14	26	22	2308	130	449	0.00777
242	10	27	1	2308	90	42	0.00722	312	14	27	2	2308	130	42	0.00287
243	10	28	6	2308	90	87	0.03011	313	14	28	5	2308	130	87	0.00080
244	10	29	11	2308	90	374	0.00997	314	14	29	24	2308	130	374	0.00831
245	10	30	5	2308	90	156	0.00723	315	14	30	9	2308	130	156	0.00145
246	11	12	22	2308	579	106	0.00831	316	15	16	0	2308	56	25	0.00000
247	11	13	19	2308	579	71	0.00212	317	15	17	6	2308	56	328	0.00612
248	11	14	32	2308	579	130	0.00112	318	15	18	28	2308	56	1050	0.00246
249	11	15	11	2308	579	56	0.00540	319	15	19	10	2308	56	295	0.00987
250	11	16	6	2308	579	25	0.00047	320	15	20	11	2308	56	277	0.01583
251	11	17	79	2308	579	328	0.00661	321	15	21	3	2308	56	81	0.01309
252	11	18	263	2308	579	1050	0.00052	322	15	22	12	2308	56	472	0.00119
253	11	19	73	2308	579	295	0.00199	323	15	23	1	2308	56	76	0.01138
254	11	20	66	2308	579	277	0.00685	324	15	24	1	2308	56	37	0.00186
255	11	21	17	2308	579	81	0.00594	325	15	25	3	2308	56	138	0.00259
256	11	22	134	2308	579	472	0.03385	326	15	26	12	2308	56	449	0.00252
257	11	23	12	2308	579	76	0.01262	327	15	27	0	2308	56	42	0.00000
258	11	24	8	2308	579	37	0.00225	328	15	28	2	2308	56	87	0.00131
259	11	25	39	2308	579	138	0.00805	329	15	29	5	2308	56	374	0.01117
260	11	26	113	2308	579	449	0.00077	330	15	30	6	2308	56	156	0.01455
261	11	27	14	2308	579	42	0.00609	331	16	17	4	2308	25	328	0.00138
262	11	28	28	2308	579	87	0.01108	332	16	18	10	2308	25	1050	0.00132
263	11	29	108	2308	579	374	0.02922	333	16	19	3	2308	25	295	0.00067
264	11	30	42	2308	579	156	0.00531	334	16	20	3	2308	25	277	0.00000
265	12	13	2	2308	106	71	0.01227	335	16	21	0	2308	25	81	0.00000
266	12	14	6	2308	106	130	0.00024	336	16	22	5	2308	25	472	0.00024
267	12	15	2	2308	106	56	0.00553	337	16	23	1	2308	25	76	0.00235
268	12	16	1	2308	106	25	0.00141	338	16	24	1	2308	25	37	0.01637
269	12	17	9	2308	106	328	0.01938	339	16	25	1	2308	25	138	0.00362
270	12	18	45	2308	106	1050	0.00322	340	16	26	5	2308	25	449	0.00031
271	12	19	12	2308	106	295	0.00550	341	16	27	1	2308	25	42	0.01312
272	12	20	7	2308	106	277	0.02165	342	16	28	0	2308	25	87	0.00000
273	12	21	5	2308	106	81	0.01251	343	16	29	3	2308	25	374	0.00284
274	12	22	30	2308	106	472	0.01848	344	16	30	3	2308	25	156	0.00849
275	12	23	1	2308	106	76	0.02429	345	17	18	155	2308	328	1050	0.00642
276	12	24	5	2308	106	37	0.03165	346	17	19	42	2308	328	295	0.00027
277	12	25	7	2308	106	138	0.00503	347	17	20	41	2308	328	277	0.00566
278	12	26	18	2308	106	449	0.00612	348	17	21	11	2308	328	81	0.00162
279	12	27	0	2308	106	42	0.00000	349	17	22	81	2308	328	472	0.03438
280	12	28	4	2308	106	87	0.00004	350	17	23	8	2308	328	76	0.00883
281	12	29	21	2308	106	374	0.01071	351	17	24	4	2308	328	37	0.00390
282	12	30	6	2308	106	156	0.00783	352	17	25	26	2308	328	138	0.02071
283	13	14	4	2308	71	130	0.00001	353	17	26	77	2308	328	449	0.03424
284	13	15	1	2308	71	56	0.01043	354	17	27	4	2308	328	42	0.00611
285	13	16	0	2308	71	25	0.00000	355	17	28	12	2308	328	87	0.00115
286	13	17	8	2308	71	328	0.00657	356	17	29	53	2308	328	374	0.00047
287	13	18	29	2308	71	1050	0.00324	357	17	30	29	2308	328	156	0.02233
288	13	19	8	2308	71	295	0.00376	358	18	19	136	2308	1050	295	0.00196
289	13	20	8	2308	71	277	0.00194	359	18	20	119	2308	1050	277	0.00760
290	13	21	2	2308	71	81	0.00626	360	18	21	33	2308	1050	81	0.00380
291	13	22	18	2308	71	472	0.00761	361	18	22	215	2308	1050	472	0.00032
292	13	23	2	2308	71	76	0.00459	362	18	23	32	2308	1050	76	0.00254
293	13	24	1	2308	71	37	0.00198	363	18	24	23	2308	1050	37	0.00597
294	13	25	3	2308	71	138	0.00931	364	18	25	70	2308	1050	138	0.00731
295	13	26	18	2308	71	449	0.00962	365	18	26	205	2308	1050	449	0.00087
296	13	27	3	2308	71	42	0.02450	366	18	27	21	2308	1050	42	0.00184
297	13	28	4	2308	71	87	0.01570	367	18	28	40	2308	1050	87	0.00042
298	13	29	16	2308	71	374	0.01240	368	18	29	180	2308	1050	374	0.01120
299	13	30	3	2308	71	156	0.01190	369	18	30	75	2308	1050	156	0.00412
300	14	15	6	2308	130	56	0.02243	370	19	20	33	2308	295	277	0.00926
301	14	16	0	2308	130	25	0.00000	371	19	21	15	2308	295	81	0.01633
302	14	17	18	2308	130	328	0.00153	372	19	22	58	2308	295	472	0.00566
303	14	18	58	2308	130	1050	0.00115	373	19	23	10	2308	295	76	0.00100
304	14	19	18	2308	130	295	0.00497	374	19	24	5	2308	295	37	0.00093
305	14	20	13	2308	130	277	0.00996	375	19	25	23	2308	295	138	0.01933
306	14	21	6	2308	130	81	0.01146	376	19	26	56	2308	295	449	0.00355
307	14	22	23	2308	130	472	0.00805	377	19	27	9	2308	295	42	0.01254
308	14	23	3	2308	130	76	0.01019	378	19	28	12	2308	295	87	0.00310
309	14	24	2	2308	130	37	0.00066	379	19	29	52	2308	295	374	0.01287
310	14	25	9	2308	130	138	0.00942	380	19	30	20	2308	295	156	0.00022

Table A1 *(continued).*

Pair	E_1	E_2	r	n	k_1	k_2	MKCI	Pair	E_1	E_2	r	n	k_1	k_2	MKCI
381	20	21	9	2308	277	81	0.00270	409	23	25	4	2308	76	138	0.00408
382	20	22	46	2308	277	472	0.02564	410	23	26	20	2308	76	449	0.01201
383	20	23	10	2308	277	76	0.00328	411	23	27	1	2308	76	42	0.00513
384	20	24	2	2308	277	37	0.00895	412	23	28	2	2308	76	87	0.01028
385	20	25	20	2308	277	138	0.01320	413	23	29	21	2308	76	374	0.02401
386	20	26	57	2308	277	449	0.00788	414	23	30	6	2308	76	156	0.00572
387	20	27	2	2308	277	42	0.01118	415	24	25	3	2308	37	138	0.00580
388	20	28	9	2308	277	87	0.00541	416	24	26	8	2308	37	449	0.00182
389	20	29	43	2308	277	374	0.00573	417	24	27	0	2308	37	42	0.00000
390	20	30	22	2308	277	156	0.01269	418	24	28	0	2308	37	87	0.00000
391	21	22	14	2308	81	472	0.00563	419	24	29	4	2308	37	374	0.00542
392	21	23	2	2308	81	76	0.00852	420	24	30	6	2308	37	156	0.02280
393	21	24	2	2308	81	37	0.00880	421	25	26	24	2308	138	449	0.00674
394	21	25	7	2308	81	138	0.01620	422	25	27	1	2308	138	42	0.01115
395	21	26	13	2308	81	449	0.00637	423	25	28	4	2308	138	87	0.00905
396	21	27	1	2308	81	42	0.00596	424	25	29	31	2308	138	374	0.02456
397	21	28	3	2308	81	87	0.00063	425	25	30	15	2308	138	156	0.03867
398	21	29	10	2308	81	374	0.00866	426	26	27	7	2308	449	42	0.00266
399	21	30	5	2308	81	156	0.00315	427	26	28	13	2308	449	87	0.00908
400	22	23	12	2308	472	76	0.00776	428	26	29	72	2308	449	374	0.00202
401	22	24	5	2308	472	37	0.00553	429	26	30	34	2308	449	156	0.00872
402	22	25	32	2308	472	138	0.00851	430	27	28	2	2308	42	87	0.00488
403	22	26	91	2308	472	449	0.00217	431	27	29	9	2308	42	374	0.00598
404	22	27	7	2308	472	42	0.00343	432	27	30	3	2308	42	156	0.00105
405	22	28	18	2308	472	87	0.00046	433	28	29	16	2308	87	374	0.00528
406	22	29	63	2308	472	374	0.03410	434	28	30	5	2308	87	156	0.00586
407	22	30	25	2308	472	156	0.01569	435	29	30	23	2308	374	156	0.00654
408	23	24	1	2308	76	37	0.00292	**Average MKCI for 30 experiments (435 pairs):**							**0.00769**

References

[1] Wang, W., Chen, T., Cai, Z., Heidari, A. A., Chen, H., & Yu, S. (2025). Gaussian-driven dynamic artemisinin optimization for feature selection in high-dimensional medical data. *Biomedical Signal Processing and Control*, *110*, 108312. https://doi.org/10.1016/j.bspc.2025.108312

[2] Yue, X., Liao, Y., Peng, H., Kang, L., & Zeng, Y. (2025). A high-dimensional feature selection algorithm via fast dimensionality reduction and multi-objective differential evolution. *Swarm and Evolutionary Computation*, *94*, 101899. https://doi.org/10.1016/j.swevo.2025.101899

[3] Zaman, E. A. K., Mohamed, A., & Ahmad, A. (2022). Feature selection for online streaming high-dimensional data: A state-of-the-art review. *Applied Soft Computing*, *127*, 109355. https://doi.org/10.1016/j.asoc.2022.109355

[4] Dhas, M. M., & Singh, N. S. (2024). Breast Cancer Diagnosis Using Majority Voting Ensemble Classifier Approach. *Journal of Soft Computing and Data Mining*, *5*(1). https://doi.org/10.30880/jscdm.2024.05.01.013

[5] Mat Rani, L., Mohd Foozy, C. F., & Mustafa, S. N. B. (2023). Feature Selection to Enhance Phishing Website Detection Based On URL Using Machine Learning Techniques. *Journal of Soft Computing and Data Mining*, *4*(1). https://doi.org/10.30880/jscdm.2023.04.01.003

[6] Nssibi, M., Manita, G., & Korbaa, O. (2023). Advances in nature-inspired metaheuristic optimization for feature selection problem: A comprehensive survey. *Computer Science Review*, *49*, 100559. https://doi.org/10.1016/j.cosrev.2023.100559

[7] Yab, L. Y., Wahid, N., & Hamid, R. A. (2022). A Meta-Analysis Survey on the Usage of Meta-Heuristic Algorithms for Feature Selection on High-Dimensional Datasets. *IEEE Access*, *10*. https://doi.org/10.1109/ACCESS.2022.3221194

[8] Kaur, S., Kumar, Y., Koul, A., & Kumar Kamboj, S. (2023). A Systematic Review on Metaheuristic Optimization Techniques for Feature Selections in Disease Diagnosis: Open Issues and Challenges. *Archives of Computational Methods in Engineering*, *30*(3), 1863–1895. https://doi.org/10.1007/s11831-022-09853-1

[9] Ahmed, A. M., & Abdulazeez, A. M. (2021). Examining Swarm Intelligence-based Feature Selection for Multi-Label Classification. *Journal of Soft Computing and Data Mining*, *2*(2). https://doi.org/10.30880/jscdm.2021.02.02.006

[10] Mujilahwati, S., Mohd Safar, N. Z., Ku Khalif, K. M. N., & Ghazalli, N. (2024). Optimizing Sentiment Analysis of Indonesian Texts: Enhancing Deep Learning Models with Genetic Algorithm-Based Feature Selection. *Journal of Soft Computing and Data Mining*, *5*(2). https://doi.org/10.30880/jscdm.2024.05.02.016

[11] Yab, L. Y., Wahid, N., & Hamid, R. A. (2023). Inversed Control Parameter in Whale Optimization Algorithm and Grey Wolf Optimizer for Wrapper-Based Feature Selection: A Comparative Study. *International Journal on Informatics Visualization*, *7*(2). https://doi.org/10.30630/joiv.7.2.1509

[12] Yab, L. Y., Wahid, N., & A Hamid, R. (2024). Improved Ozone Level Detection through Feature Selection with Modified Whale Optimization Algorithm. *Qubahan Academic Journal*, *4*(1), 265–276. https://doi.org/10.48161/qaj.v4n1a466

[13] Chakraborty, S., Saha, A. K., Ezugwu, A. E., Chakraborty, R., & Saha, A. (2023). Horizontal crossover and co-operative hunting-based Whale Optimization Algorithm for feature selection. *Knowledge-Based Systems*, *282*. https://doi.org/10.1016/j.knosys.2023.111108

[14] Fang, L., & Liang, X. (2023). A Novel Method Based on Nonlinear Binary Grasshopper Whale Optimization Algorithm for Feature Selection. *Journal of Bionic Engineering*, *20*(1), 237–252. https://doi.org/10.1007/s42235-022-00253-6

[15] Yab, L. Y., Wahid, N., & A Hamid, R. (2024). Impact of Balanced Exploration and Exploitation on Highdimensional Feature Selection with Hierarchical Whale Optimisation Algorithm. *Journal of Information and Communication Technology*, *23*(4), 593–626. https://doi.org/10.32890/jict2024.23.4.2

[16] Reddy, K., & Saha, A. K. (2022). A modified Whale Optimization Algorithm for exploitation capability and stability enhancement. *Heliyon*, *8*(10), e11027. https://doi.org/10.1016/j.heliyon.2022.e11027

[17] Yab, L. Y., Wahid, N., & Hamid, R. A. (2022). A Modified Whale Optimization Algorithm as Filter-Based Feature Selection for High Dimensional Datasets. In *Lecture Notes in Networks and Systems: Vol. 457 LNNS*. https://doi.org/10.1007/978-3-031-00828-3_9

[18] Wang, F., Feng, S., Pan, Y., Zhang, H., Bi, S., & Zhang, J. (2023). Dynamic spiral updating whale optimization algorithm for solving optimal power flow problem. *Journal of Supercomputing*, *79*(17), 19959–20000. https://doi.org/10.1007/s11227-023-05427-5

[19] *Dataset: RNA-Seq*. (n.d.). [Dataset]. UCI Machine Learning Repository. Retrieved June 30, 2025, from https://archive.ics.uci.edu/dataset/401/gene+expression+cancer+rna+seq

[20] *Dataset: Lung (Dana-Farber Cancer Institute, Harvard Medical School)*. (n.d.). [Dataset]. ELVIRA Biomedical Data Set Repository. Retrieved June 30, 2025, from https://leo.ugr.es/elvira/DBCRepository/LungCancer/LungCancer-Harvard1.html

[21] *Dataset: Lymphoma DLBCL (Stanford University)*. (n.d.). [Dataset]. Kent Ridge Bio-medical Data Set Repository. Retrieved June 30, 2025, from https://web.archive.org/web/20080126151255/http://sdmc.lit.org.sg/GEDatasets/Datasets.html#DLBCL

[22] *Dataset: SRBCT (Khan et al.)*. (n.d.). [Dataset]. Bioinformatics Laboratory of University of Ljubljana. Retrieved June 30, 2025, from https://figshare.com/articles/dataset/SRBCT_data/6527348?file=11995805

[23] *Dataset: Colon (Princeton University)*. (n.d.). [Dataset]. Kent Ridge Bio-medical Data Set Repository. Retrieved June 30, 2025, from https://web.archive.org/web/20080126151255/http://sdmc.lit.org.sg/GEDatasets/Datasets.html#Colon Tumor

[24] Theng, D., & Bhoyar, K. K. (2023). Feature selection techniques for machine learning: A survey of more than two decades of research. *Knowledge and Information Systems*. https://doi.org/10.1007/s10115-023-02010-5

[25] Mirjalili, S., & Lewis, A. (2016). The Whale Optimization Algorithm. *Advances in Engineering Software*, *95*, 51–67. https://doi.org/10.1016/j.advengsoft.2016.01.008

[26] Mirjalili, S., Mirjalili, S. M., & Lewis, A. (2014). Grey Wolf Optimizer. *Advances in Engineering Software*, *69*, 46–61. https://doi.org/10.1016/j.advengsoft.2013.12.007

[27] Anuar, M. A., Ibrahim, R., Zainal, N., Rejab, M., & Hachimi, H. (2025). A Comparative Study of Metaheuristic Optimization Algorithms on Distinct Benchmark Functions. *Journal of Soft Computing and Data Mining*, *6*(1), 69–85. https://doi.org/10.30880/jscdm.2025.06.01.005

[28] Wu, X., Zhang, S., Xiao, W., & Yin, Y. (2019). The Exploration/Exploitation Tradeoff in Whale Optimization Algorithm. *IEEE Access*, *7*, 125919–125928. https://doi.org/10.1109/ACCESS.2019.2938857

[29] Wald, R., Khoshgoftaar, T. M., & Napolitano, A. (2013). Stability of filter- and wrapper-based feature subset selection. *Proceedings - International Conference on Tools with Artificial Intelligence, ICTAI*, 374–380. https://doi.org/10.1109/ICTAI.2013.63

[30] Metz, C. E. (1978). Basic principles of ROC analysis. *Seminars in Nuclear Medicine*, *8*(4), 283–298. https://doi.org/10.1016/S0001-2998(78)80014-2